A fragility-oriented approach for seismic retrofit design

Karim Aljawhari[1], Roberto Gentile[2] , and Carmine Galasso, M.EERI[1,2]

Abstract

This study proposes a practical fragility-oriented approach for the seismic retrofit design of case-study structures. This approach relies on mapping the increase of the global displacement-based ratio of capacity to life-safety demand (CDR_{LS}) to the building-level fragility reduction. Specifically, the increase of CDR_{LS} due to retrofitting is correlated with the corresponding shift in the fragility median values of multiple structure-specific damage states, observing that a pseudo-linear trend is appropriate under certain conditions. Accordingly, a practical approach is proposed to fit such a (structure-specific) linear trend and then use it by first specifying the desired fragility median and subsequently finding the corresponding target value of CDR_{LS} that must be achieved through retrofit design. The validity of the proposed approach is illustrated for an archetype reinforced concrete (RC) structure not conforming to modern seismic design requirements, which has been retrofitted using various techniques, namely, fiber-reinforced polymers wrapping of columns and joints, RC jacketing, and steel jacketing.

Keywords

Seismic retrofit, fragility analysis, retrofit design, reinforced concrete, performance-based earthquake engineering

Date received: 26 May 2021; accepted: 14 January 2022

Introduction

Many existing reinforced concrete (RC) buildings in earthquake-prone regions do not conform to modern seismic design codes as they were designed/built to resist gravity loads only. As a result, those structures are vulnerable to severe damage or even collapse under moderate-to-high ground-shaking intensity levels (e.g. De Luca et al., 2018). This has led to significant economic and life losses, as demonstrated by numerous past earthquakes (e.g. Mazzoni et al., 2018; Ricci et al., 2011; Stewart et al., 2018). Structural retrofit is often

[1]Scuola Universitaria Superiore Pavia (IUSS), Pavia, Italy
[2]University College London (UCL), London, UK

Corresponding author:
Carmine Galasso, University College London (UCL), Gower Street, London WC1E 6BT, UK.
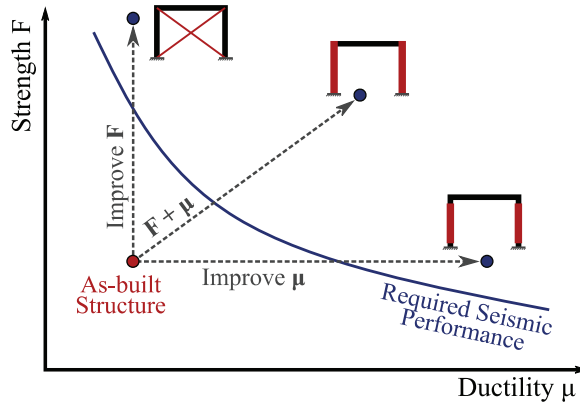Email: c.galasso@ucl.ac.uk

Figure 1. Effects of different retrofit strategies on seismic performance.

necessary to mitigate the consequences of earthquakes on such buildings and improve their seismic performance. This approach has become quite popular in recent times due to ease of construction and cost-effectiveness compared with other drastic solutions like demolition and replacement. In general, retrofit strategies aim to either modify key structural properties such as strength, ductility, and stiffness—as depicted in Figure 1—or reduce seismic demand. Several techniques (systems) can be used to achieve one or more strategies. For instance, adding RC shear walls (e.g. Kaplan et al., 2011; Miano et al., 2017) or bracing (e.g. Badoux and Jirsa, 1990; Freddi et al., 2013, 2021; Gutiérrez-Urzúa et al., 2021) to existing buildings notably improves stiffness and lateral strength. In contrast, base isolation is applied to reduce seismic demand by decoupling the horizontal motion of a structure and that of the ground (e.g. Natale et al., 2021).

Many challenges may arise in adopting the above techniques. Those challenges are related to the architectural compatibility of the intervention, its invasiveness, the need to modify existing foundations or add new ones, the high implementation costs, and long work duration. Therefore, less-invasive retrofit techniques are more widespread. Examples include wrapping structural elements with fiber-reinforced polymers (FRP) and jacketing columns using steel or RC jackets, which enhance ductility and/or strength. These local techniques are fundamentally less expensive, and they pose a minimal degree of invasiveness/business interruption compared with RC shear walls or bracing. It should be noted that structural retrofit can improve lateral sway mechanisms of buildings, especially if they experience non-ductile local sway ones (e.g. joint failure, soft story). Such mechanisms can be shifted to global ones such as mixed sway, where plastic hinges develop in different structural elements (e.g. beams, columns, joints), or even beam sway, where plastic hinges only form in beams and column bases.

While retrofitted structures are generally expected to perform better against earthquake-induced ground shaking, field observations for such buildings under actual seismic events are still scarce (O'Reilly and Sullivan, 2018). This indicates the lack of sufficient empirical seismic fragility and vulnerability models in the literature, which are essential for applications aimed to select/design/implement seismic risk reduction strategies and ultimately enhance the resilience of earthquake-prone communities. This also demonstrates the need to derive such models numerically adopting nonlinear dynamic analysis

methods, which usually require a large number of analyses, practically incompatible with the preliminary/conceptual design process. Moreover, especially in the seismic risk assessment of building portfolios, retrofit solutions are often designed based on engineering judgment using simplified models without accounting for different alternatives and/or performance objectives. Such a practice does not grant an analyst the complete control over the reduction in seismic fragility/loss estimates and makes it challenging to optimize the results.

Accordingly, a practical and relatively flexible approach is needed to fill this gap, enabling one to control and specify the desired seismic fragility level and returning the corresponding "nominal" performance to be achieved through retrofit design. Such a "nominal" performance is usually assessed by using simple metrics quantified within the acceleration–displacement response spectrum (ADRS) space, thus requiring pushover-based analysis methods. One common metric is the displacement-based global ratio of capacity to life-safety (LS) demand of a similar new structure (CDR_{LS}), or simply capacity–demand ratio (New Zealand Society for Earthquake Engineering (NZSEE), 2006).

The above issues have attracted many research efforts in the past few decades, but a limited number of studies are available. Although a detailed review of such studies is beyond the scope of this article, a few are briefly discussed to provide the reader with some background on the topic. Most of the past research focused on the experimental investigation of different retrofit techniques and developing analytical and numerical models to simulate their effect on existing structural elements and/or systems. For instance, some studies investigated the effects of steel jackets on RC columns experimentally and developed design procedures (e.g. Aboutaha et al., 1996, 1999; Alvarez et al., 2018; Priestley et al., 1994), while others explored FRP retrofitting (e.g. Alvarez et al., 2018; Lam and Teng, 2003; Priestley and Seible, 1995; Seible et al., 1997) and RC jacketing for columns (e.g. Priestley et al., 1996; Rodriguez and Park, 1994).

On the contrary, some studies developed fragility relationships considering FRP, RC jacketing, base isolation, and adding shear walls (e.g. Cardone et al., 2019; Liel and Deierlein, 2013). However, the fragility relationships in these studies accounted for collapse only, without considering other damage states (DSs), which may significantly contribute to earthquake-induced losses for low-to-moderate ground shaking levels. Moreover, the retrofit solutions in some studies were either applied based on engineering judgment, that is, without appropriately accounting for structure-specific seismic deficiencies or specific performance objectives (e.g. Liel and Deierlein, 2013), or considering solely one, rather than different, performance objective (e.g. Cardone et al., 2019; Gentile and Galasso, 2021b). Contrarily, other studies considered applying different retrofit techniques with varying intervention levels to achieve various performance objectives (e.g. Harrington and Liel, 2021; Ligabue et al., 2018), but only collapse fragility relationships were evaluated. These studies also attempted to map different performance metrics to decision variables of interest, such as collapse risk and/or seismic losses, to provide insight into their correlation.

Based on the aforementioned discussion, the current study proposes a practical fragility-oriented approach based on mapping the increase of CDR_{LS} due to retrofitting to the reduction of building-level seismic fragility. The proposed approach enables the selection of the desired fragility level and returns the required "nominal" structural performance in terms of CDR_{LS}. This approach informs the retrofit design process, connecting the desired level of fragility to the corresponding CDR_{LS}, which is easy to control in the

preliminary/conceptual retrofit design phase. It is worth mentioning that, under certain assumptions, the desired level of fragility can be directly linked to seismic risk estimates/loss metrics (as discussed later in the article), thus allowing the designer to effectively control such metrics through fragility reduction. After conceptualizing the proposed fragility-oriented retrofit design approach, this study demonstrates its validity using a case-study archetype RC frame located in a high-seismicity zone, which has been retrofitted using three different techniques: FRP wrapping, steel jacketing, and RC jacketing. The results are finally discussed to draw some remarks and recommendations for further research.

Fragility-oriented retrofit design

For this study, the nominal seismic performance of a structure of interest is quantified using CDR_{LS}; that is, the displacement-based global ratio of capacity to LS seismic demand. The LS demand is calculated by first transforming the force–deformation relationship (i.e. capacity curve) derived from pushover analysis to a capacity spectrum of an equivalent single-degree-of-freedom (SDoF) system plotted in the acceleration–displacement space. The capacity spectrum method (CSM) is then applied to obtain the "nominal" structural performance (Applied Technology Council (ATC)-40, 1996; Freeman, 1998). In contrast, a more-rigorous characterization of the improvement in seismic performance is obtained through fragility relationships, which provide the likelihood of exceeding different DSs over a range of ground-shaking intensity levels. However, the derivation of such relationships could be very time-consuming and computationally expensive because it usually requires carrying out nonlinear time-history analyses (NLTHAs) for a large set of ground-motion records.

Retrofit generally aims to reduce seismic risk (for instance, in terms of the expected annual loss, EAL) to an acceptable level. Computing seismic risk, however, requires quantifying site-specific seismic hazard, fragility relationships, and damage-to-loss models. Since retrofit will mainly affect fragility estimates, it might be required to design numerous retrofit solutions, derive fragility relationships (based on NLTHA) for each one, and then evaluate the seismic risk until meeting the target level. Such a process can be quite impractical and/or infeasible. To tackle this issue, this study proposes a fragility-oriented approach that allows specifying the desired fragility level, represented by the median of the fragility relationship for a given DS (μ_{DS}) before the retrofit design. One can then obtain the corresponding CDR_{LS} value that must be achieved through retrofit design to ensure the desired level of fragility is satisfied.

The proposed approach relies on the practical assumption that the relationship between CDR_{LS} and μ_{DS} for a given structure is pseudo-linear when its performance is improved via retrofitting. This trend can be empirically inferred from past results (e.g. Aljawhari et al., 2021; Harrington and Liel, 2021). Such a trend can also be demonstrated on theoretical grounds under specific conditions. For pre-collapse DSs (e.g. life safety, near-collapse), it is common to adopt the popular power-law model ($EDP = aIM^b$) to characterize the probabilistic seismic demand model in terms of an engineering demand parameter (EDP) (e.g. maximum drift) and a ground-motion intensity measure (IM). The slope factor of this model (a) generally relies on the stiffness of the structure, while the power factor (b) is close to 1.0 (Cornell et al., 2002; Jalayer et al., 2017). This indicates that the power-law model tends to be linear for any DS less severe than collapse. Accordingly, if the
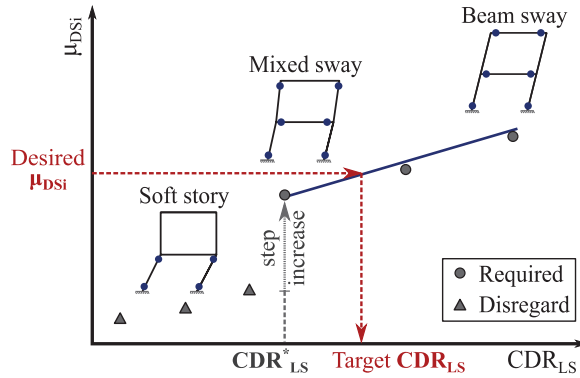
Figure 2. Schematics of the CDR_{LS} versus μ_{DS} linear fit.

stiffness of the retrofitted structure is similar to that of the as-built one, the increase in CDR_{LS} will correspond to an improvement in the displacement capacity, and thus, a nearly linear increase in μ_{DS}.

To apply the proposed fragility-oriented approach, it is practically required to obtain only three points in the CDR_{LS} versus μ_{DS} space, and then derive the linear best fit as per Figure 2. The first point can refer to the as-built structure itself, but this is only permitted when the stiffness of the retrofitted structure changes smoothly while CDR_{LS} increases (i.e. no major shift in the plastic mechanism). The slope of the power-law model, in this case, will not change abruptly, and a single linear model describing the CDR_{LS} versus μ_{DSi} relationship becomes effective. This case can be specifically encountered if the as-built structure exhibits a global mixed-sway mechanism. The remaining two points refer to any retrofit solutions with considerably higher CDR_{LS} but not necessarily conforming to any specific performance objectives. One of those points can be a beam-sway configuration (obtained by inverting the local hierarchy of strength at each beam–column joint), while the other could be any arbitrary point between the previous two.

Conversely, if the as-built structure shows an unfavorable local mechanism (i.e. soft-story), the retrofit design will likely aim to shift this mechanism to a beam-sway, or at least a mixed-sway one. Such a mechanism shift leads to an abrupt change in the slope of the power-law model, which appears as a step increase in the CDR_{LS} versus μ_{DSi} relationship (at CDR_{LS}^*) that becomes, in turn, a piecewise linear relationship as shown in Figure 2. In such a case, two different linear models (in theory) can be, respectively, fitted before and after CDR_{LS}^*. The first branch of this piecewise linear relationship is arguably not needed for design purposes as it is undesirable to adopt a retrofit solution leading to a soft-story behavior. Therefore, the first point to be used in deriving the linear best-fit should represent a retrofit solution that shifts the local mechanism of the as-built structure to a global one. The remaining two points are defined as explained previously.

Upon properly defining the three points and considering the above discussion, a linear model can be fitted for each DS, as shown in Figure 3. Those CDR_{LS} versus μ_{DSi} models can be used by first specifying the desired level of fragility median for any DS (Step 1) and then locating the intersection point on the corresponding model (Step 2). Next, a vertical line can be extended from this point until it intersects the fitted models for the other DSs (if their medians are needed) and the horizontal axis (Steps 3–5). These new intersections
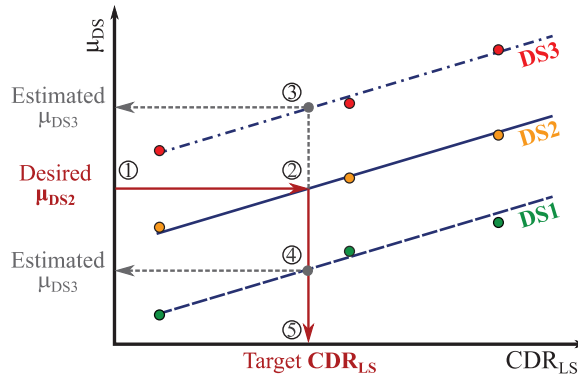
Figure 3. Conceptual illustration of the fragility-oriented approach for retrofit design.

represent the estimated fragility median values for the other DSs and the target CDR_{LS} needed for the final fragility-oriented retrofit design. Finally, after finishing the design of a suitable retrofit solution that achieves the target CDR_{LS}, NLTHA can be performed to re-derive fragility relationships if more accuracy is needed.

It is important to recall that the CDR_{LS} values of the three points selected for fitting the linear models are determined using pushover analysis only. On the contrary, the required fragility parameters (i.e. μ_{DSi}) associated with each DS should be derived based on NLTHA. However, to reduce the needed computational effort at this stage, those parameters might be alternatively derived by using simplified response analysis approaches. Procedures such as the cloud-CSM (e.g. Nettis et al., 2021) may provide a beneficial trade-off between accuracy and efficiency. Capacity curves in this procedure are derived via pushover analyses (or "by-hand" approaches such as the Simple Lateral Mechanism Analysis, SLaMA), and IM versus EDP clouds are generated via the CSM to derive fragility relationships (e.g. Gentile and Galasso, 2021a).

It is worth emphasizing that the desired fragility level specified at the start of the proposed approach can correspond to an acceptable level of risk/loss (e.g. EAL). In fact, the specified fragility level, combined with a damage-to-loss model and a site-specific seismic hazard, can be used to compute the resulting EAL. This can be finally compared with acceptable values selected by the designer. This check must be assured before evaluating the target CDR_{LS} and proceeding with the retrofit design. The EAL can also be assessed along with other decision variables (e.g. implementation costs, functional compatibility) using multi-criteria decision-making schemes (e.g. Caterino et al., 2008; Gentile and Galasso, 2021b). This, in turn, makes the proposed fragility-oriented approach helpful for guiding the design of optimal retrofit solutions. The proposed approach can be additionally adopted in retrofit plans of building portfolios, particularly when the modeled buildings are carefully selected to be representative of typical classes/archetypes in a given portfolio, as it will be possible to obtain template retrofit configurations for the selected classes/archetypes.

Finally, the proposed approach can also be advantageous to facilitate budget and resource allocation procedures needed for risk mitigation of building portfolios, mainly if the limited availability of financial resources constrains the decision-making process. This can be achieved by optimizing the levels of fragility that provide the best reduction in the
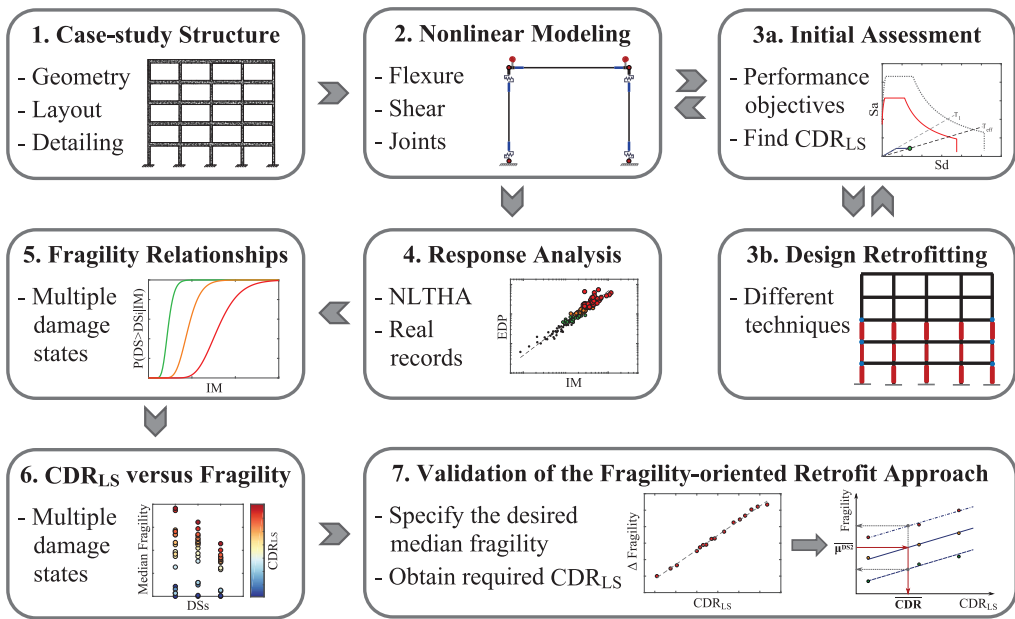
Figure 4. Flowchart for the analysis of the case-study structure and validation of the proposed fragility-oriented approach for retrofit design.

overall seismic risk within the available budget and resources. Furthermore, the proposed fragility-oriented approach could be applied oppositely. Specifically, an analyst can design a retrofit solution, perform a pushover analysis to find the corresponding CDR_{LS} and then use the linear models of CDR_{LS} versus μ_{DSi} to provide reasonable estimates of the median values of fragility for any DS without performing NLTHAs. This is especially useful when dealing with large building portfolios that include a few typical building classes.

Case-study application

The appropriateness of the linear models characterizing the CDR_{LS} versus μ_{DSi} relationship, as well as the applicability of the fragility-oriented approach for retrofit design, are demonstrated by analyzing a case-study non-ductile RC frame. The adopted workflow is depicted in Figure 4, and it incorporates the following steps: identification of a case-study structure (Step 1); developing advanced numerical models to simulate the non-linear response of both the as-built and retrofitted case-study structures (Step 2); design of multiple retrofit solutions to meet specific performance objectives (Step 3); performing cloud-based NLTHA using a selected set of unscaled ground-motion records (Step 4); derivation of fragility relationships (Step 5); analysis of CDR_{LS} versus median fragility (μ_{DSi}) correlation (Step 6). The outcome of Step 6 is used to validate the proposed fragility-oriented approach for retrofit design (Step 7).

Case-study building

An older five-story, four-bay RC moment-resisting frame with a total height of 15 m and a uniform bay width of 4.5 m is considered, as shown in Figure 5. This frame is designed to resist gravity loads only according to the Royal Decree n. 2229 in Italy in 1939 (Consiglio
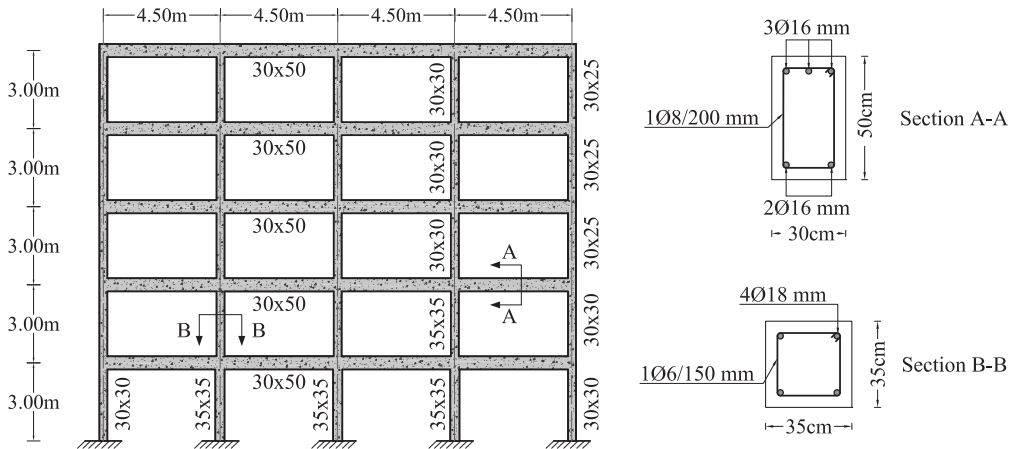
Figure 5. Layout of the case-study frame and sample cross sections (section dimensions are in centimeters).

dei Ministri, 1939), which regulated the design of RC frames until 1974. Following this decree, simulated design (e.g. Verderame et al., 2010) is performed to define the proportioning and detailing of the structural elements, using the allowable stress design.

It should be noted that buildings designed according to this decree constitute a considerable portion of RC structures in Italy. For instance, Rosti et al. (2021) investigated more than 2400 RC residential buildings in L'Aquila and Irpinia to derive empirical fragility relationships. They found that almost all buildings in Irpinia were built before the seismic classification in 1981, thus they were designed for gravity loads only. In contrast, most of the RC buildings in L'Aquila were built after the seismic classification in 1915, indicating that they have some seismic resistance. However, almost 35% of those were designed before 1981, i.e., using obsolete building codes that do not adopt modern seismic design requirements (Rosti et al., 2021). Similar observations were indicated by Del Gaudio et al. (2017) for L'Aquila upon investigating more than 7500 RC buildings. It is also interesting to note that 67% of L'Aquila's considered buildings are mid-rise (three to five stories), whereas around 33% of the residential RC structures in Irpinia belong to such a category (Del Gaudio et al., 2017; Rosti et al., 2021).

Clearly, the frame resulting from the simulated design does not satisfy the modern seismic design provisions, such as capacity design and strong column–weak beam. Beams and columns are poorly confined, and those have a very low amount of longitudinal rebar (less than 1%). Moreover, the joints lack transverse reinforcement, use smooth bars, and improper anchorage (Calvi et al., 2002a, 2002b; Pampanin et al., 2002). This makes the frame susceptible to forming brittle failure mechanisms such as soft story, joint, and shear failure. Typical average values for the material properties are used, which are representative of that era. Specifically, the average concrete compressive strength (f_{cm}) is 16.5 MPa, in compliance with other studies (e.g. Braga et al., 2001; Masi et al., 2014). The average yield strength (f_{ym}) of reinforcing steel is equal to 330 MPa (e.g. Caprili et al., 2012; Puppio et al., 2017; Verderame et al., 2001).

Considered retrofit techniques

Three retrofit techniques are investigated in this study: FRP wrapping, steel jacketing, and RC jacketing. Typical cross sections for columns retrofitted using these techniques are

illustrated in Figure 6. FRP wrapping is used here to retrofit joints and columns to prevent any shear failure. It also provides a high level of confinement for columns, thus improving their ductility under extreme load conditions (e.g. Priestley and Seible, 1995; Seible et al., 1997). The contribution of FRP wrapping to the lateral stiffness and flexural strength is minimal because the unidirectional fibers are placed perpendicular to the longitudinal axis of columns.

The selected FRP material consists of laminated precured sheets with high-strength carbon fibers (CFRP), which are wrapped around the full height of as-built columns. This type is among the most commonly used ones in the practice and literature (e.g. Alvarez et al., 2018; Cardone et al., 2019; Harrington and Liel, 2020, 2021; Natale et al., 2021). The elasticity modulus (E_f) is equal to 140 GPa, (average) ultimate tensile strength (F_{fu}) is 2000 MPa, and rupture strain (ε_{fu}) is 1.2% (American Concrete Institute (ACI) 440.2R, 2008; National Research Council (CNR)-DT 200 R1/2013, 2013). Each FRP layer is 0.5-mm-thick, and the maximum number of layers is equal to five to ensure confinement efficiency (CNR-DT 200 R1/2013, 2013). It should be noted that the FRP is also used for joint retrofitting in the cases where joint failure is observed (mainly in external ones).

Rectangular and elliptical steel jackets are another popular option to prevent the shear failure of columns. They can also increase lateral stiffness due to the isotropic steel properties (Alvarez et al., 2018). However, only elliptical (or circular) jackets are used in this study because they effectively improve confinement and ductility due to the continuous confining pressure they provide (Priestley et al., 1994). This technique can also offer some enhancement of flexural strength. Conversely, experiments demonstrated that rectangular steel jackets lose much of their confinement efficiency (e.g. Priestley et al., 1994, 1996). The adopted steel jacketing consists of full-height elliptical/circular jackets. The space between the jacket and retrofitted column can be filled with grout material or plain concrete (e.g. Alvarez et al., 2018; Priestley et al., 1994). The jackets are made of structural steel grade S235 with an average yield strength (f_{yj}) of 235 MPa and a minimum thickness equal to 1.5 mm (e.g. Harrington and Liel, 2020). A gap of 50 mm is deliberately left between the edges of the steel jacket and foundations/beams to prevent excessive flexural strength enhancement, which transfers forces to adjacent members (Priestley et al., 1994).

RC jacketing is the most traditional and common technique in practice as it is characterized by a low cost and does not require specialized labor. It consists of encasing existing columns with a cast-in-place RC jacket to improve confinement, ductility, and both shear and flexural strengths. Continuous column jacketing in two consecutive floors also enhances joint behavior. The thickness of an RC jacket is mainly controlled by the size of longitudinal and transverse reinforcement to be used, in addition to the minimum cover requirement (e.g. Lizundia et al., 2006; Priestley et al., 1996). Compared with the other two techniques, RC jacketing poses the highest level of invasiveness. It can notably increase the size of existing columns and may require extending reinforcement through slabs, foundations, and joints. The adopted RC jacketing involves a full-height encasement of existing columns using cast-in-situ concrete, with the possibility of extending longitudinal rebar through foundations and slabs. RC jackets with a minimum thickness of 50 mm are adopted, with at least 4Φ14 mm for external columns and 4Φ16 mm for internal ones (Φ refers to the diameter). Hoops with Φ8 mm are used with a spacing not exceeding 150 mm. The concrete material is characterized by f_{cm} of 33 MPa, while f_{ym} for the reinforcement is 490 MPa.
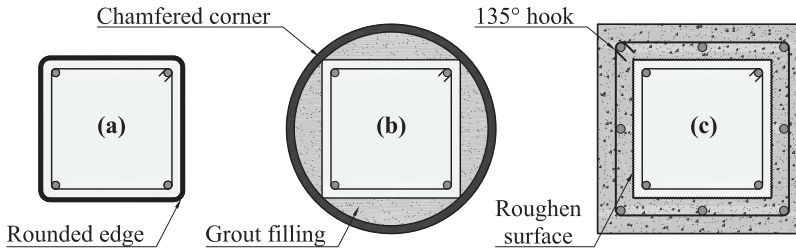
Figure 6. Typical cross sections of a column retrofitted using (a) FRP, (b) steel, and (c) RC jacketing.

Damage-state definition

Three structure-specific DSs are adopted to characterize different damage conditions reflecting the building's performance level (PL). Each DS occurs when the structure attains a specific threshold defined with respect to an EDP. This study adopts the maximum interstory drift ratio (MIDR) as an EDP, which is a reliable and widely used proxy to quantify global structural and nonstructural damage (at least for drift-sensitive components). The MIDR thresholds for each DS are calibrated by assessing multiple measurable criteria during pushover analysis using a modal-pattern incremental load. These criteria are adapted from Aljawhari et al. (2020) and summarized in Table 1. θ_y and θ_u are the yield and ultimate chord rotations, respectively. The latter is evaluated according to Eurocode 8-Pt.3 (EN 1998-3, 2005). It must be noted that the MIDR threshold for each DS is based on the first occurrence of any criterion among those shown in Table 1 (e.g. Aljawhari et al., 2020).

The three selected DSs are defined as follows: DS1 reflects moderate damage levels; DS2 represents significant damage (SD); and DS3 accounts for near-collapse conditions. Buildings experiencing DS2 and DS3 should meet the life safety and collapse-prevention PLs, respectively. A more detailed description of each DS is provided in Table 1. Since the infills are not modeled explicitly, the defined DSs do not account for the initial infill damage. However, it is possible to indirectly tackle this issue by using predefined MIDR thresholds existing in different codes/standards that account for such damage (e.g. 0.5%). Lastly, it should be noted that the analytical formulation of θ_u requires inputting the amount of transverse reinforcement. This is directly applicable for existing structural components and those retrofitted using RC jackets. In the case of FRP and steel jacketing, the equivalent transverse reinforcement concept is implemented (e.g. Alvarez et al., 2018;

Table 1. Criteria adopted for mapping of DSs: Aljawhari et al. (2020)

Level/DS	DS1	DS2	DS3
Section level	Reaching yield bending in a supporting column	Max. bending strength of a column is reached	Reaching shear failure in any element
Component level	Reaching θ_y in any supporting column	Reaching 75% of the θ_u in any component	Reaching the θ_u in any component
Global level	Reaching the global yield point of the structure	Reaching the maximum strength	About 20% drop in the maximum strength
General description	Moderate structural and nonstructural damage. No significant yielding of members	Severe structural and nonstructural damage. Some residual strength and stiffness is retained	Full exploitation of strength and ductility. Low residual strength and stiffness

DS: damage state.

Harrington and Liel, 2020, 2021). In this approach, the FRP or steel jacketing can be converted to standard transverse reinforcement that mimics their effect by generating a lateral confining pressure equal to that produced by either of them.

Performance-targeted retrofit design

In this study, a large number of retrofit configurations (realizations) with varying performance are developed to demonstrate the linear trend between CDR_{LS} and μ_{DSi} considering different performance objectives (performance-targeted retrofitting). For each objective, a specific PL (or DS) under a defined hazard level (e.g. American Society of Civil Engineers (ASCE)/SEI 41-17, 2017) must be achieved, which can be investigated by using the CSM and evaluating the CDR_{LS} value. An iterative design procedure is adopted to develop the different retrofit configurations for each technique. Design iterations might vary with respect to the detailing, geometric characteristics, and number of retrofitted elements, resulting in numerous realizations of potential retrofitted structures with incremental improvement in their seismic performance. It is worth highlighting that the large number of retrofitted structures developed in this study is only needed to validate the hypothesis of the linear relationship between CDR_{LS} and μ_{DSi}. In contrast, the proposed fragility-oriented retrofit design approach requires defining only three retrofit configurations, as discussed above.

For the sake of simplicity, the same hazard level is used for all performance objectives, which is the one associated with life safety, that is, corresponding to a 475-year mean return period (e.g. EN 1998-3, 2005). The seismic demand corresponding to this hazard level, which is used to design/assess the different retrofitted cases developed in this study, is characterized by a Type-1 response spectrum as per Eurocode 8 (EN 1998-1, 2004). This spectrum is defined adopting a peak ground acceleration (PGA) of 0.30 g and a ground type C to account for high seismicity conditions. Such a code-based demand is adopted for convenience and practicality; however, analysts can use any other demand form. A summary of the adopted performance objectives is provided in Table 2. Some performance objectives, other than those listed in Table 2, might require using different hazard levels with return periods lower than 475 years (e.g. operational performance objective), but they are outside of the scope of this article.

It should be noted that the 475-year hazard level, introduced above, is selected because it is the most relevant and widely used one for the design/assessment of building structures, especially in Europe—and for which hazard maps/curves are (generally) readily available. It is interesting to note that, for US-based buildings, the same hazard level existed in FEMA 356 (Federal Emergency Management Agency (FEMA), 2000). However, other

Table 2. Selected performance objectives for seismic retrofit

Performance objective	Description
No-(near)collapse performance	Achieve the collapse-prevention PL (DS3) against the LS seismic demand
Limited performance	Partially achieve significant damage PL (DS2) against LS demand ($CDR_{LS} \approx 75\%$)
Basic performance	Achieve the significant-damage PL (DS2) against LS demand (100% of CDR_{LS})
Advanced performance	Achieve moderate damage (DS1; limited occupancy) against LS seismic demand

PL: performance level; DS: damage state; LS: life-safety.

hazard levels are currently implemented in the most recent standards, particularly ASCE/ SEI 41-17 (2017), depending on the performance objective (e.g. 225- and 975-year hazard level for the basic performance objective).

Nonlinear-modeling strategies

The nonlinear response of the case-study building is simulated by developing 2D numerical models via OpenSees (McKenna, 2011). Structural components are modeled as beam–column elements with finite-length plastic hinges to simulate the nonlinear flexural response, which is defined by performing moment–curvature analysis following Priestley et al. (2007) and Karthik and Mander (2011). The hysteretic parameters and post-capping degrading response for the moment–curvature are based on O'Reilly and Sullivan (2019). Additional shear springs are added in series to the beam–column elements to account for potential shear failure modes, as shown in Figure 7a. The backbone curve parameters for the shear response are calculated following Mergos and Kappos (2012), Sezen and Moehle (2004), and Zimos et al. (2015).

As stated earlier, joints in older Italian RC frames lack transverse reinforcement and use smooth bars with end-hooks, mainly in external ones (e.g. Calvi et al., 2002a, 2002b; Pampanin et al., 2002). Therefore, the early failure of such joints leads the building to develop a brittle failure mechanism. Thus, an additional spring is added in each beam–column joint zone, as indicated by Figure 7b. The parameters of the nonlinear material used for joints are defined according to O'Reilly and Sullivan (2019); a mechanics-based approach introduced in many other studies (e.g. Pampanin et al., 2003; Priestley, 1997).

It is acknowledged that the response of RC frames in Italy (and the Mediterranean region) can be considerably influenced by the presence of infills. However, they are not considered explicitly in the adopted modeling strategy. Despite such a limitation, disregarding infills remains a very popular simplification in the design practice for new structures and existing ones if they need retrofit intervention. Nevertheless, it might be necessary to consider infills in fragility analyses, at least to confirm that the fragility is reduced (right-shifting of fragility relationships) or to investigate the effects of infills on the lateral sway mechanism of retrofitted buildings. Furthermore, considering infills becomes essential if higher accuracy is needed, particularly when evaluating risk-related decision variables such as seismic losses. This is because the infill damage represents the major contributor to such losses, especially at low-intensity levels of ground shaking (e.g. Cardone and Perrone, 2015; De Risi et al., 2018; Del Gaudio et al., 2019; Sassun et al., 2016).
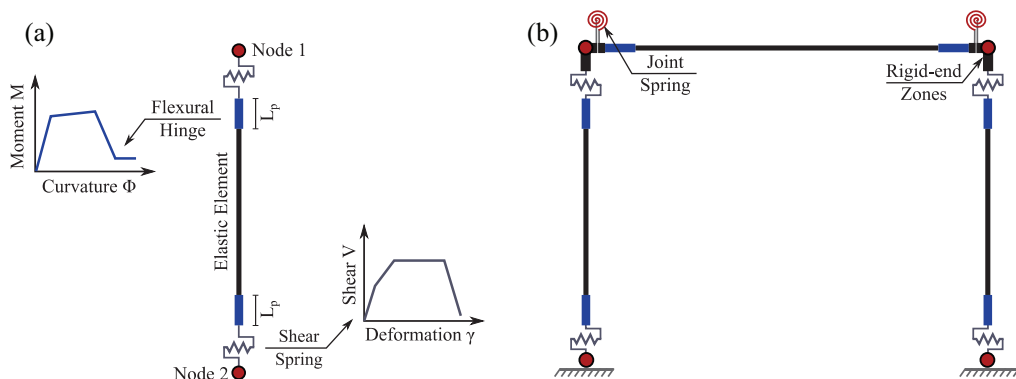

Figure 7. (a) Modeling strategy for column elements and (b) modeling of a frame configuration.

To account for the FRP effects on columns, the moment–curvature relationship is modified considering the confinement provided by this technique. This is achieved by first assuming that the entire column's cross section is confined, rather than the core only, since FRP layers are wrapped around the external perimeter of the column. Next, the confinement pressure (f_l) due to FRP wrapping is calculated based on Priestley and Seible (1995) and then the compressive strength and ultimate strain of the confined concrete (f_{cc} and ε_{ccu}) are estimated based on Mander et al. (1988) and Priestley and Seible (1995), respectively. It should be noted that FRP wrapping around rectangular columns is less effective than circular ones because only inward corner forces provide the confinement in the former case instead of continuous pressure around the perimeter. Thus, a confinement effectiveness factor is used to reduce the value of f_l as per ACI 440.2R (2008). Moreover, the additional shear strength due to FRP is calculated and added to the value of the as-built column following Priestley and Seible (1995).

It should also be noted that the unique failure modes pertaining to FRP, such as debonding and fracture mechanisms, are not explicitly modeled, assuming the FRP retrofit is designed and installed appropriately so that the concrete and reinforcement will govern the softening behavior of the elements at high levels of deformation (e.g. Harrington and Liel, 2020, 2021). Steel jacketing is treated similarly to FRP. The value of f_l is estimated as per Priestley et al. (1994), while f_{cc} and ε_{ccu} are found based on Mander et al. (1988) and Priestley et al. (1996), respectively. These new values are adopted to modify the moment–curvature relationship. The additional shear strength due to the steel jacket is estimated according to Priestley et al. (1994). Finally, columns retrofitted with RC jackets are treated as equivalent monolithic members. This assumption is valid if the jackets are well constructed and the surface of existing columns is adequately treated (e.g. Bousias et al., 2007; Harrington and Liel, 2020). However, to address the possibility of a poor bond between RC jackets and existing columns, the as-built value of f_c is used for the entire cross section, and it is assumed that lateral confinement is provided solely by the hoops of the new RC jacket (Priestley et al., 1996).

Fragility relationships and ground-motion record selection

Retrofit can lead to a significant improvement in fragility relationships, which describe the conditional probability of exceeding different structure-specific DSs over a range of IM levels, that is, $P(DS \geqslant DSi|IM)$. Such relationships can be derived using the cloud analysis approach that includes selecting a set of unscaled ground-motion records covering a wide range of IM levels to run NLTHA (Jalayer et al., 2015). Other approaches involving stepped scaling of records can also be used in fragility derivation, such as the multiple-stripe analysis (MSA) (Jalayer and Cornell, 2009) and incremental dynamic analysis (Vamvatsikos and Cornell, 2002), but they are outside the scope of this study. The cloud analysis approach generates IM versus EDP clouds that can be adopted to fit probabilistic seismic demand models (PSDMs) in the form of a power-law ($EDP = aIM^b$), which eventually allows deriving fragility relationships using a closed-form solution (Cornell et al., 2002). The adopted fragility derivation approach accounts explicitly for the collapse analysis cases via the method proposed by Jalayer et al. (2017). The collapse corresponds to the global dynamic instability of the numerical analysis and/or maximum interstory drift values (Jalayer et al., 2017) larger than a nominal threshold (e.g. 10%). The formulation of $P(DS \geqslant DSi|IM)$ is reported by Equations 1 and 2:

$$P(DS \geqslant DSi|IM) = P(DS \geqslant DSi|IM, NC)(1 - P(C|IM)) + P(DS \geqslant DSi|IM, C)P(C|IM) \quad (1)$$

$$P(DS \geqslant DSi|IM, NC) = \Phi\left(\frac{\ln(IM/\mu_{DSi|NC})}{\beta_{DSi|NC}}\right) \quad (2)$$

where C and NC account for the collapse and non-collapse cases; $P(C|IM)$ is the probability of collapse (given an IM value) characterized by a generalized regression model with a "logit" link function (logistic regression); $P(DS \geqslant DSi|IM, NC)$ is the conditional probability of exceeding a specific DS given an IM level, and given that collapse has not taken place; $P(DS \geqslant DSi|IM, C)$ is equal to 1.0 as all DSs are exceeded if collapse has taken place. $\mu_{DSi|NC}$ and $\beta_{DSi|NC}$ are, respectively, the median and dispersion of the fragility relationships evaluated for the NC cases only. As done in Gentile and Galasso (2020), the parameters of the final distribution (including C and NC cases) are the median, that is, μ_{DSi}, equal to that in Equation 1, and the logarithmic standard deviation (β_{DSi}) calculated as per Equation 3, in which $IM_{16/84}$ are the 16th and 84th percentiles of the original distribution. The β_{DSi} is constant for all DSs for each set of fragility relationships due to the homoscedasticity assumption adopted in cloud analysis:

$$\beta = \frac{[\ln(IM_{84}) - \ln(IM_{16})]}{2} \quad (3)$$

The records used for NLTHA are selected from the SIMBAD (*Selected Input Motions for Displacement-based Assessment and Design*) database developed by Smerzini et al. (2014), which includes 467 three-component records of shallow crustal earthquakes with magnitudes from 5 to 7.3 and epicentral distances less than 30 km (Smerzini et al., 2014). Only 150 records are selected following the criteria defined in Gentile and Galasso (2021b) and Gentile et al. (2019) to reduce computational efforts yet maintain the engineering significance of analysis. Specifically, all ground motions are ranked based on their PGA obtained as the geometric mean of the two horizontal components. The horizontal component with the highest PGA is kept for each ground motion, then the 150 records with the highest rank are selected. Such a record-selection procedure is compatible with the adopted analysis approach, that is, cloud analysis. This approach, among others such as the MSA, is more appropriate for risk assessment of building portfolios, especially when coupled with optimal IMs, as done in this study. This is related to the fact that it does not require site- and building-specific hazard-consistent record selection; thus, the same record set can be used to perform NLTHAs for an entire building portfolio.

The implemented IM is the geometric mean of the 5%-damped spectral acceleration over a specific range of periods (*avgSa*), which indirectly accounts for the effects of higher modes and period elongation due to component damage and strength/stiffness degradation (e.g. Baker and Cornell, 2006; Kazantzi and Vamvatsikos, 2015; Kohrangi et al., 2017). This IM type, compared with conventional ones like the spectral acceleration at the fundamental period $Sa(T_1)$, minimizes response variability and has a higher relative sufficiency (e.g. Minas and Galasso, 2019; O'Reilly, 2021). It should be noted that the *avgSa* is calculated considering 10 equally spaced periods ranging between $0.2T_1$ and $1.5T_1$ (e.g. Kohrangi et al., 2016). However, to allow the fragility comparison between the as-built and the retrofitted cases, the same period range is adopted for all of them, which is based on T_1 of the as-built case. This assumption is considered valid since the change in T_1 for the majority of retrofitted cases is not substantial.

Results and discussion

Performance assessment for the as-built structure

To understand the response and failure mechanism of the as-built case-study structure, an initial assessment is carried out using pushover analysis to identify the DS thresholds and then apply the CSM to evaluate the CDR_{LS} before any retrofit intervention. It should be noted that the equivalent viscous damping needed to apply the CSM is calculated following the Takeda-Fat hysteretic rule, as recommended by Priestley et al. (2007) for RC frames. Figure 8a shows the pushover curve with the horizontal axis representing the MIDR (mainly dominated by the third-story deformation), and the vertical axis showing the base shear. The first occurrence of some damage observations is also illustrated in Figure 8a, such as the first yield for beams and columns, SD for columns and joints (θ_{SD} and γ_{SD}), and joint failure (γ_u); mainly external ones. The MIDR thresholds for all DSs are listed in Table 3, in addition to relevant information on the dynamic characteristics of the structure, that is, T_1 and the mass participation ratio.

It can be observed in Figure 8a that both DS2 and DS3 are controlled by the limit states of the joints, which take place before those of the columns. It is also noticed that the beams do not reach their θ_{SD} and θ_u despite their initial yielding. The nonlinear behavior is mostly concentrated in the columns and joints at the third story. Accordingly, retrofit efforts must be directed toward improving the key properties (i.e. strength, ductility, stiffness) of these structural components in particular, which will eventually improve the overall plastic mechanism of the building until achieving a beam-sway one (mainly characterized by beam hinging).

Figure 8b illustrates the idealized capacity spectrum of the equivalent SDoF system and the demand spectrum, both elastic and inelastic, plotted in the ADRS space. Applying the CSM, it is found that the inelastic demand spectrum (for a damping level corresponding to the LS displacement) significantly exceeds the capacity of the as-built structure. In other words, the capacity spectrum cannot intersect the inelastic demand spectrum, thus indicating a CDR_{LS} less than 1.0. According to Figure 8b, the maximum capacity corresponds to a spectral displacement (Sd) equal to 0.07 m. However, the expected displacement demand identified through the intersection between the secant-to-LS stiffness line and the inelastic demand spectrum is equal to 0.167 m. Therefore, the CDR_{LS} of the as-built structure is equal to 42%, demonstrating the need for structural retrofit.
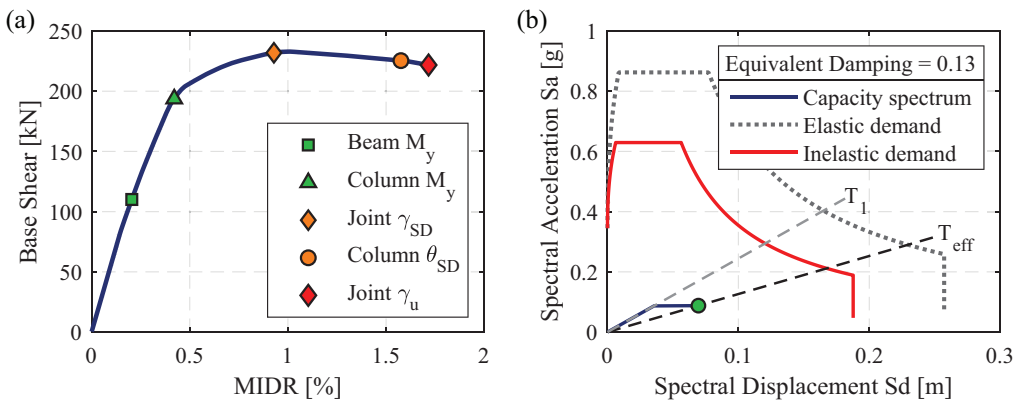

Figure 8. As-built case: (a) pushover curve and damage observations and (b) capacity and demand spectra.

Table 3. MIDR thresholds for different DSs derived from pushover analysis

Damage state (DS)	DS1	DS2	DS3
MIDR thresholds (%)	0.41	0.93	1.71
Fundamental period T_1 (s)	1.33 (82% mass participation)		

DS: damage state; MIDR: maximum interstory drift ratio.
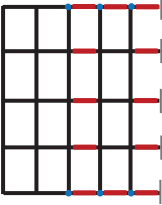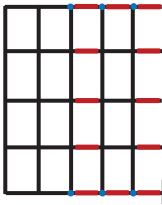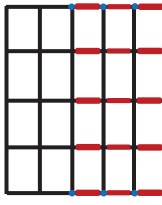
Designed retrofitting solutions

The as-built structure is retrofitted aiming at selected performance objectives (see Table 2) to study the CDR_{LS} versus μ_{DSi} correlation. The iterative design process resulted in 13 retrofitted cases using FRP wrapping of columns and joints, 15 cases for steel jacketing, and cases 18 for RC jacketing. It should be noted that any change in the dynamic characteristics (e.g. mass, stiffness, T_1) due to retrofit was explicitly reflected in the pushover analysis, modal load pattern, and CSM. The MIDR thresholds of the various DSs were also re-computed to consider any capacity improvement.

Table 4 shows the details, layout, and number of retrofitted elements using FRP for all performance objectives. For brevity, only one retrofitted case is described for each performance objective, particularly the one satisfying the objective with the minimum possible amount of intervention. Table 4 demonstrates that the advanced performance objective could not be achieved using the FRP wrapping because it only improves ductility through confinement and increases shear strength. Its contribution to the lateral strength and stiffness is minimal (less than 10% in this study). However, enhancing these parameters is essential with respect to moderate damage PL (or DS1) as the columns will not yield quickly, especially at low IM levels. It should be noted that the maximum value of CDR_{LS} that could be achieved is 110%, obtained using five FRP layers for the columns. Adding more layers would be ineffective and will not improve the performance.

Table 5 provides similar information about the cases retrofitted with steel jacketing. It was possible to generate many cases of retrofitted buildings with larger CDR_{LS} values compared with the FRP case, particularly up to 147%. Such an observation can be primarily attributed to the high effectiveness of circular/elliptical jackets with respect to the high and continuous (radial) confinement they provide. This, in turn, significantly improves the ductility of the columns, thus making them capable of sustaining considerable levels of inelastic deformation. This also enhances the (near) collapse condition, allowing the beams to undergo failure before columns. Similarly to the FRP case, all these advantages are insufficient to make the structure experience moderate damage (DS1) against the LS demand (i.e. the advanced performance objective) for the same reasons explained previously.
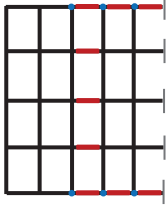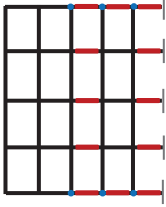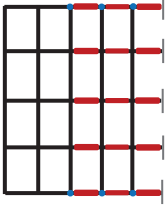
Finally, a summary of the case studies with RC jacketing is provided in Table 6, which shows that the advanced performance objective is achieved, unlike FRP and steel jacketing. This is because the RC jacketing provides a significant overall enhancement for the stiffness and strength, both shear and flexural, and improves the ductility through confinement. These features can also shift the building mechanism from local (e.g. soft-story) to global, that is, beam-sway. Therefore, the (frame-level) MIDR threshold of DS1 becomes much higher, and the retrofitted structure will not be easily subjected to yielding and moderate damages, especially at low IM levels. Nevertheless, as illustrated in Table 6, achieving the advanced PL requires retrofitting the entire columns of the case-study building, resulting in a global retrofit intervention rather than local, which might be expensive and technically challenging.

Table 4. Description of FRP retrofit solutions for different performance objectives

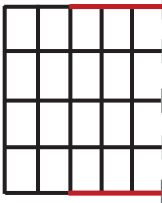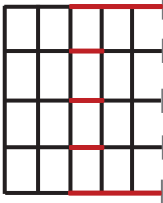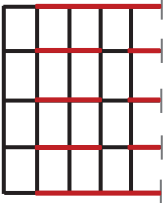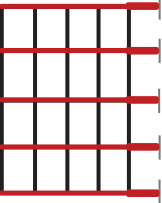| Performance objective	T_1 (s)	CDR_{LS}(%)	Description of FRP retrofitting	Graphical illustration
No-collapse performance	1.33	65	One layer for external columns and joints in the 1st to 3rd floor and one layer for internal columns in the 1st and 3rd floors	
Limited performance	1.32	76	Same joint retrofitting as above. Two layers for the 3rd floor columns and internal columns of the 1st floor. One layer for external columns in 1st to 2nd floor	
Basic performance	1.31	105	Same joint retrofitting as above. One layer for the 2nd floor columns. Four layers for the 1st floor and internal columns in 3rd floor and five layers for the 3rd floor external columns	
Advanced performance	NA	NA	NA	NA

FRP: fiber-reinforced polymers.

Table 5. Description of steel jacketing retrofit solutions for different performance objectives

Performance objective	T_1 (s)	CDR_{LS} (%)	Description of steel jacketing retrofitting	Graphical illustration
No-collapse performance	1.31	61	1.5-mm-thick jacket mm for the external columns in 1st to 3rd floor and internal ones in the 3rd floor. Also retrofit external joints in 1st to 3rd floors using FRP.	
Limited performance	1.29	80	Same joint retrofitting as above. Use 1.5-mm-thick jacket for the external columns in the 1st to 3rd floor and internal ones in the 1st and 3rd floor	
Basic performance	1.27	106	Same joint retrofitting as above. 1.5-mm-thick jacket for the columns of 2nd floor. 2.5-mm-thick jackets for the 3rd floor and external columns of 1st floor. 3-mm jacket for the internal columns in 1st floor	
Advanced performance	NA	NA	NA	NA

FRP: fiber-reinforced polymers.

Table 6. Description of RC jacketing retrofit solutions for different performance objectives

| Performance objective	T_1 (s)	CDR_{LS} (%)	Description of RC jacketing retrofitting	Graphical illustration
No-collapse performance	1.26	65	Retrofit external columns in the 1st to 3rd floor with 50 mm jacket with 4Φ14 mm bars and 1Φ8/150 mm hoops	
Limited performance	1.22	78	50 mm jackets for the external columns in the 1st to 3rd floor with 4Φ14 mm bars and 1Φ8/150 mm hoops. 50 mm jackets for the internal columns of the 3rd floor with 4Φ16 mm bars and 1Φ8/150 mm hoops	
Basic performance	1.14	105	50 mm jackets for the external columns in the 1st to 4th floor with 4Φ14 mm bars and 1Φ8/150 mm hoops. 50 mm jackets for the internal columns in 1st, 3rd, 4th floors with 4Φ16 mm bars and 1Φ8/150 mm hoops	
Advanced performance	0.94	181	100 mm jackets with 8Φ16 mm bars and 1Φ8/100 mm hoops for external, and with 12Φ22 mm bars and 1Φ10/80 mm hoops for the internal columns of 1st floor. 50 mm jackets with 8Φ20 mm bars and 1Φ8/150 mm hoops for external and with 8Φ22 mm bars and 1Φ8/150 for the internal columns of 2nd floor. 50 mm jackets with 8Φ14 mm bars and 1Φ8/150 mm hoops for the 3rd, 5th and external columns of 4th floor. Similar jackets but with 8Φ16 mm bars for internal columns of the 4th floor	

RC: reinforced concrete.
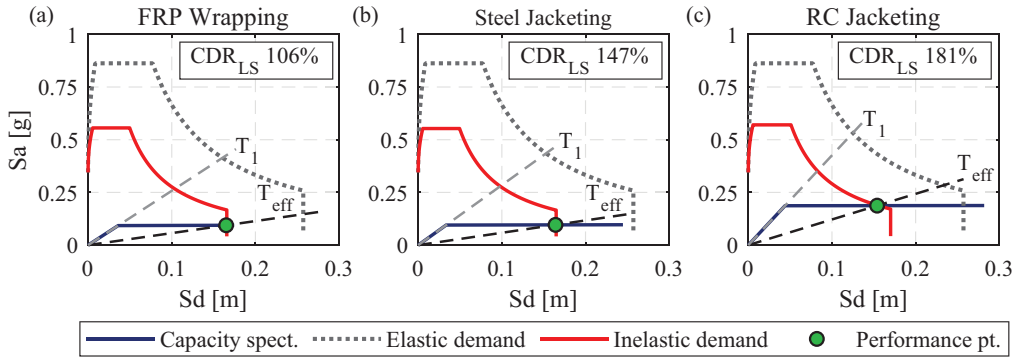
Figure 9. Capacity and demand spectra: (a) FRP wrapping, (b) steel jacketing, and (c) RC jacketing.
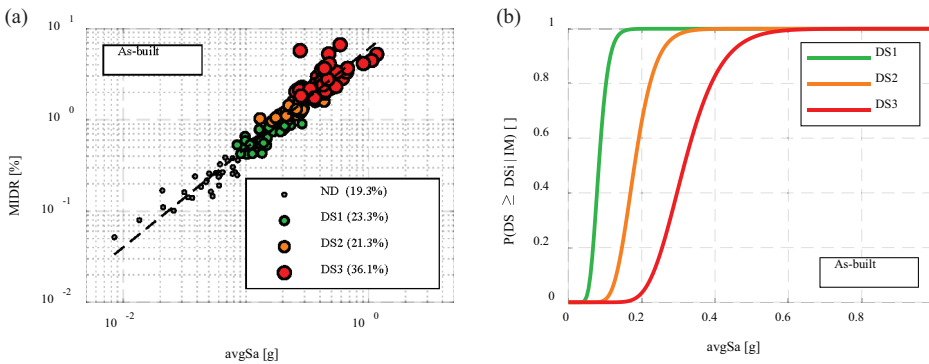

Figure 10. (a) IM versus EDP cloud and (b) fragility relationships for the as-built structure.

To provide more illustration, Figure 9 depicts the new performance points representing the intersection between demand and capacity spectra (obtained using the CSM) for a sample of retrofitted case-study structures for the three retrofit techniques considered in the current study. The corresponding values of CDR_{LS} are also provided.

Seismic fragility assessment

Upon developing non-linear models for both the as-built and retrofitted case studies, NLTHAs are performed using the selected set of ground-motion records in order to assess the seismic performance and derive the corresponding fragility relationships. Figure 10a shows the IM versus EDP cloud and the fitted PSDM, demonstrating that the as-built structure remained undamaged (ND) in less than 20% of the analysis cases. In contrast, approximately 60% of the cases are characterized by high damage conditions (i.e. DS2 and DS3). Such a poor seismic performance is also reflected in the fragility relationships in Figure 10b, showing that the building is expected to experience high DSs, even at a low IM level. Fragility assessment is then carried out considering the retrofitted case studies defined earlier. The fragility relationships for the as-built and retrofitted cases are reported in Figure 11 as evidence of the substantial impact of retrofitting. For each retrofit technique, the fragility relationships for only one retrofitted case are illustrated for each
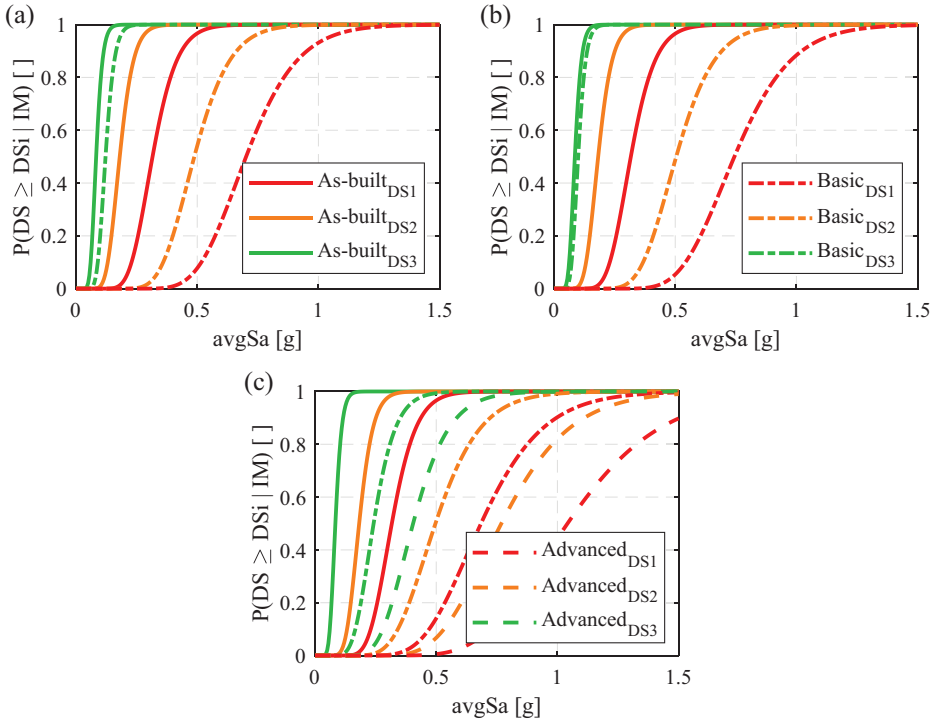
Figure 11. Fragility relationships for different performance objectives considering (a) FRP wrapping, (b) steel jacketing, and (c) RC jacketing.

Table 7. Fragility parameters of the as-built and retrofitted cases for different performance objectives

Performance	As-built	Basic			Advanced
Technique	Non-retrofitted	FRP wrapping	Steel jacketing	Concrete jacketing	Concrete jacketing
DSi	μ_{DSi} (g)	μ_{DSi} (g)	μ_{DSi} (g)	μ_{DSi} (g)	μ_{DSi} (g)
DS1	0.083	0.123	0.099	0.250	0.410
DS2	0.180	0.491	0.510	0.504	0.772
DS3	0.316	0.707	0.744	0.701	1.055
β	0.250	0.238	0.247	0.290	0.286

FRP: fiber-reinforced polymers; DS: damage state.

performance objective, particularly those that satisfied each objective with minimal intervention. The resulting fragility parameters, including median (μ_{DSi}) and dispersion (β), are summarized in Table 7.

Figure 11 reveals a significant improvement in the fragility relationships of DS2 and DS3 when the frames are retrofitted until satisfying the basic performance objective ($CDR_{LS} \approx 100\%$), which is represented by the rightward shift. This improvement is very similar for the three retrofit techniques but slightly higher for both steel and RC jacketing. However, Figures 11a and b demonstrate that the improvement in fragility relationships of DS1, unlike DS2 and DS3, is relatively low when the frames are retrofitted using either

FRP or steel jacketing. This can be explained by the fact that both techniques mainly enhance the ductility through confinement and prevent shear failure, which is beneficial for DS2 and DS3 as they are associated with the nonlinear response under high levels of inelastic deformation.

On the contrary, improving the DS1 fragility relationship requires enhancing both lateral strength and stiffness to control the sway mechanism of the building and make it more resistant against developing moderate damages due to early yielding. However, the contribution of steel jacketing to the lateral strength and stiffness is minor compared with RC jacketing, whereas the contribution of FRP is almost negligible. In contrast, RC jacketing can change the mechanism to a full beam-sway one. It also provides a significant overall improvement for all the above parameters, which resulted in a considerable shift in the DS1 fragility relationship illustrated in Figure 11c. Furthermore, the advanced performance objective could be achieved using RC jacketing, which caused a considerable shift in the fragility relationships of the three DSs.

It is important to remember that the same period range is adopted to quantify avgSa for the as-built and retrofitted cases to allow fragility comparison. This period range is based on T_1 of the as-built case, which is the largest. It is understood that T_1 might notably change upon retrofitting due to stiffness and/or mass variations. However, the retrofitted cases are more ductile than the as-built ones, and they can experience period elongation of up to $3 T_1$ (ASCE/SEI 7-16, 2017; Baker and Cornell, 2006). Also, the change in T_1 for the majority of the retrofitted cases is not substantial. This makes the selected period range appropriate for derived the fragility curves. It is also worth noting that the variation in β for the retrofitted cases, compared with the as-built case, is within 15% (see Table 7), yet allowing for a better comparison between the different fragility relationships. This minimal variation is registered as the same record set is used for every retrofit configuration, thus maintaining the same uncertainty related to record-to-record variability. Hence, the slight variation in β is attributed to the differences in dynamic response and number of collapse cases, which reduce moving from the as-built to the retrofitted cases.

Correlation between CDR_{LS} and fragility medians

The proposed fragility-oriented approach for the retrofit design relies on the assumption that the CDR_{LS} versus μ_{DSi} trend is linear. To prove this, Figure 12 shows the scatter of such data for each considered retrofit realization and retrofit technique. The same
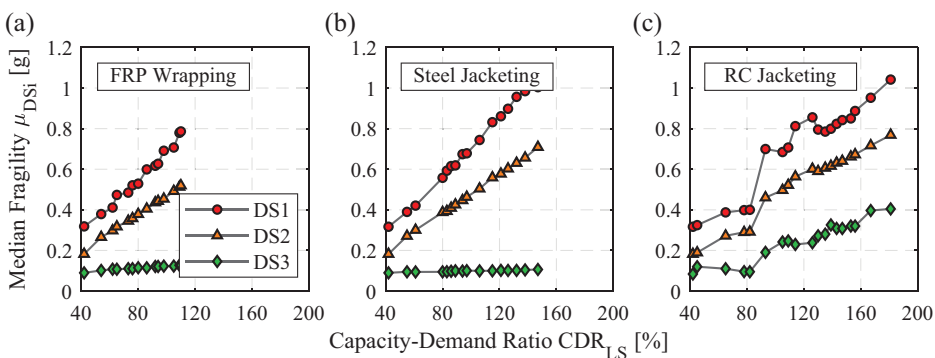

Figure 12. Variation of μ_{DS} versus CDR_{LS} for (a) FRP wrapping, (b) steel jacketing, and (c) RC jacketing.

variation is depicted in Figure 13, but this time treating μ_{DSi} in a normalized fashion, that is, considering the variation in μ_{DSi} as a percentage of μ_{DSi} of the as-built structure ($\Delta\mu_{DSi}$). A gradual increase in the values of μ_{DSi} for DS2 and DS3 is observed for all the retrofit techniques, which results from the performance improvement characterized by the CDR_{LS}. A step-change in the values of μ_{DSi} can be noted in Figures 12c and 13 for the RC jacketing, particularly for CDR_{LS} values close to 90%. As described above theoretically, such a jump is related to the sudden shift from a local to a global failure mechanism.

In contrast, the overall increase in μ_{DS} of DS1 is minimal for both FRP and steel jacketing, as clarified in Figures 12a and b and 13, even at very high levels of CDR_{LS} as discussed earlier. Only the RC jacketing is capable of significantly improving the μ_{DSi} for DS1, indicating that the structure becomes less susceptible to moderate damage, especially at low IM levels. It should also be noticed that large values of CDR_{LS} could be reached using either steel or RC jacketing. After these levels, retrofitting might become ineffective because the global failure becomes associated with the beams rather than the columns and/or joints. Contrarily, the extent of the CDR_{LS} increase in the case of the FRP technique is notably lower since a limited number of layers can be wrapped around columns to ensure confinement efficiency, as stated earlier.

The clear trends between CDR_{LS} and $\Delta\mu_{DSi}$ (or μ_{DSi}), as shown earlier, indicate that simple linear models expressing $\Delta\mu_{DSi}$ as functions of CDR_{LS} can be reasonably identified through establishing the best-fit lines in a least-square sense. Figure 14 illustrates these models for all DSs and retrofit techniques. For the RC jacketing technique only, additional piecewise linear fits are provided to reflect the observed shift in the lateral-sway mechanism. The coefficient of determination (R^2) values are also displayed, confirming the goodness of such linear fits. Although this illustrative analysis involves only a single case study, the resulting empirical data agree well with the general mechanics-based discussion about the pseudo-linear trend between CDR_{LS} and μ_{DSi} anticipated above. Therefore, it is reasonable to expect that this trend applies with some level of generality to RC frames, provided that fragility relationships are derived using the power-law model, and CDR_{LS} is displacement-based. Conservatively, applications to other structural systems/materials should be verified on a case-by-case basis.

The numerical form of the models is provided in Table 8, knowing that the initial CDR_{LS} is 42% for the FRP wrapping and steel jacketing, while it is equal to 93% for the RC jacketing, accounting for the second branch of the piecewise linear function. The proposed simplified models can be easily implemented to provide reasonable estimates for the shift in fragility relationships of the as-built structure as a result of structural retrofit once the CDR_{LS} is determined by just performing a pushover analysis. The outcome of these simplified models is directly used to modify the median values of the original fragility relationships to achieve the desired shift. This approach is deemed a quick and reasonable approximation for the preliminary/conceptual design phase instead of performing computationally expensive NLTHAs to derive new fragility relationships in a trial-and-error design procedure.

It is worth mentioning that the results obtained by the proposed models are limited by the uncertainties associated with the modeling assumptions, material properties, geometry, layout, and so on. Therefore, additional research is required to generalize such models (expressions) to other structural typologies with different failure mechanisms and geometric and material properties. Those, in turn, can be adopted to analyze and/or design scenario-based retrofit implementation plans at a portfolio level through a regional seismic risk model (e.g. Silva et al., 2018). This is beyond the scope of this study and requires further investigation.
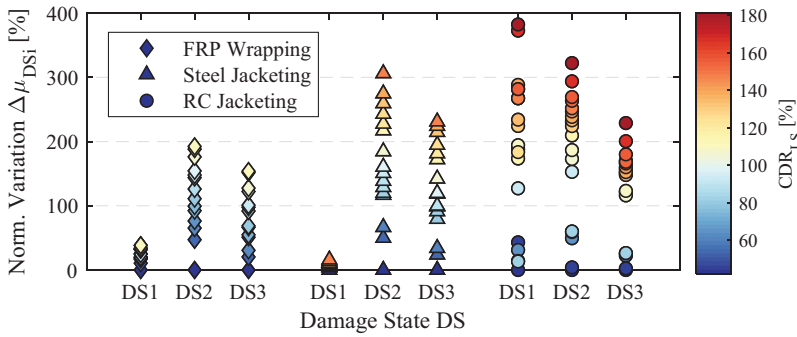
Figure 13. Variation of (μ_{DS}) versus CDR_{LS} considering the three retrofit techniques.
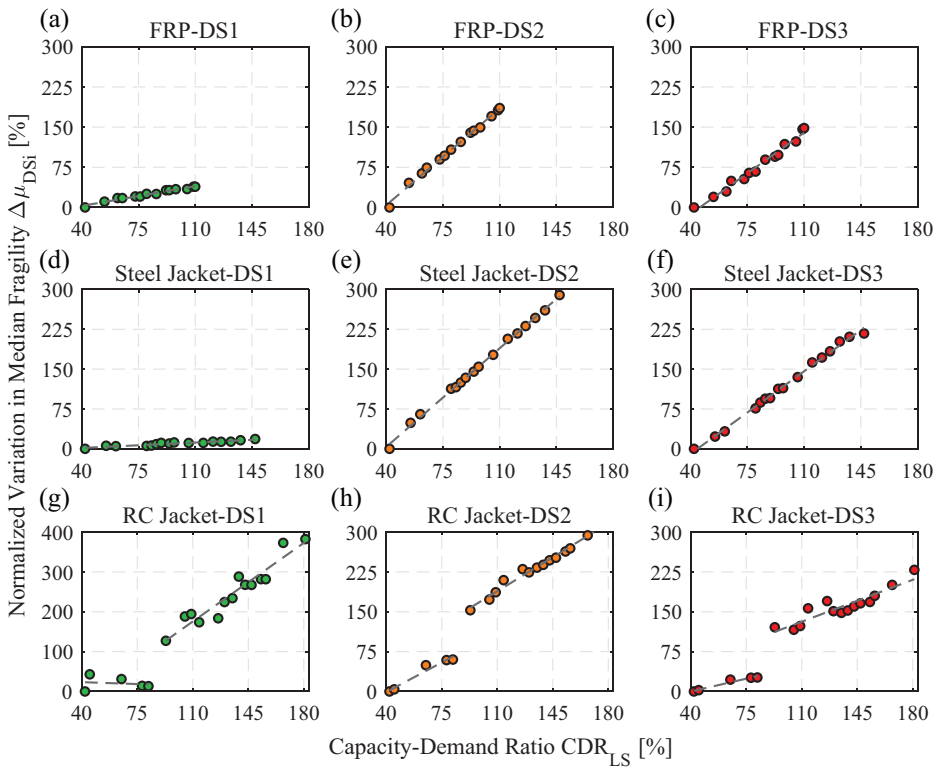

Figure 14. Correlation between the normalized variation of μ_{DS} and CDR_{LS} for all DSs and techniques: (a) $R^2 = 0.97$, (b) $R^2 = 1.00$, (c) $R^2 = 0.98$, (d) $R^2 = 0.90$, (e) $R^2 = 1.00$, (f) $R^2 = 1.00$, (g) $R^2 = 0.91$, (h) $R^2 = 0.98$, and (i) $R^2 = 0.84$.

Table 8. Mathematical expressions developed for $\Delta\mu_{DSi}$ (%) as a function of CDR_{LS}

Technique/DS	$\Delta\mu_{DS1}$ (%)	$\Delta\mu_{DS2}$ (%)	$\Delta\mu_{DS3}$ (%)
FRP wrapping	$0.524\ CDR_{LS} - 18.07$	$2.575\ CDR_{LS} - 98.69$	$2.167\ CDR_{LS} - 98.81$
Steel jacketing	$0.146\ CDR_{LS} - 4.275$	$2.650\ CDR_{LS} - 102.32$	$2.216\ CDR_{LS} - 97.79$
RC jacketing	$2.817\ CDR_{LS} - 134.29$	$1.826\ CDR_{LS} - 12.26$	$1.126\ CDR_{LS} + 7.49$

FRP: fiber-reinforced polymers; DS: damage state; RC: reinforced concrete.

An illustrative application of the fragility-oriented approach for retrofit design

The proposed fragility-oriented approach for the retrofit design takes advantage of the pseudo-linear relationship between the CDR_{LS} and μ_{DSi} (or $\Delta\mu_{DSi}$) discussed earlier and further demonstrated in the previous section. Therefore, only three points are sufficient to fit a line expressing this relationship (for each DS) with a reasonable level of accuracy. Analysts can adopt the proposed approach by (1) selecting the desired level of μ_{DSi} for any DS; (2) obtaining estimations of μ_{DSi} for the other DSs; and finally (3) obtaining the CDR_{LS} value to be achieved through retrofit design to ensure that the desired fragility levels are satisfied (see Figure 3). For illustrative purposes, fitting such lines using only three points is performed for each retrofit technique. This is accomplished by selecting random three-point sets, finding the best-fit lines, and then comparing them with the models fitted using the entire set of points.

It is worth recalling that if the retrofit intervention leads to a significant shift in the sway mechanism (e.g. from soft-story to beam-sway), the relationship between CDR_{LS} and μ_{DSi} will be piecewise linear. The first branch of this piecewise linear relationship, as explained earlier, can be completely disregarded as it is not desirable to design any retrofit intervention leading to a local soft-story mechanism. This situation was observed in the RC jacketing case since a shift in the plastic mechanism took place, as indicated in Figure 15. The figure also reports the fitted linear models using both the complete set of points and a three-point set selected after the mechanism shift.

It is interesting to note in Figure 15 that the models fitted by using the three-point set upon the mechanism shift are almost identical to those fitted using the entire point set, which incorporates all the different mechanisms simultaneously. This is attributed to the fact that most of the points in the full set constitute the retrofitted structures after the mechanism shift, so they dominated the fitted models. However, for practical application of the fragility-oriented approach, only three points are needed for efficiency. Therefore, special attention must be given to the failure mechanism for each selected point. On the contrary, the FRP wrapping and steel jacketing techniques could not entirely prevent column hinging; hence, no sudden jump was recorded in the CDR_{LS} versus μ_{DSi} space. Therefore, the linear models fitted using a three-point set with the as-built configuration as the first point, as shown in Figure 16a, would be similar to those fitted using the mixed-
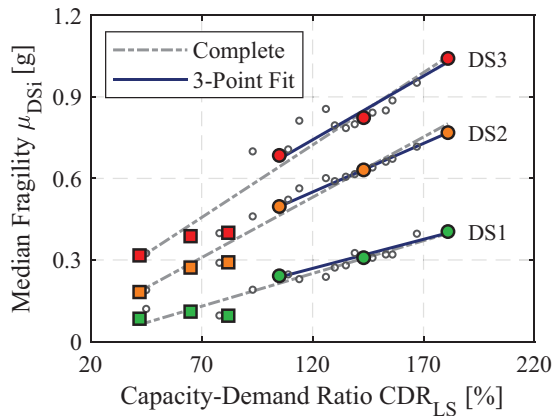

Figure 15. Linear models of CDR_{LS} versus μ_{DSi} for RC jacketing fitted via a full and a three-point set.
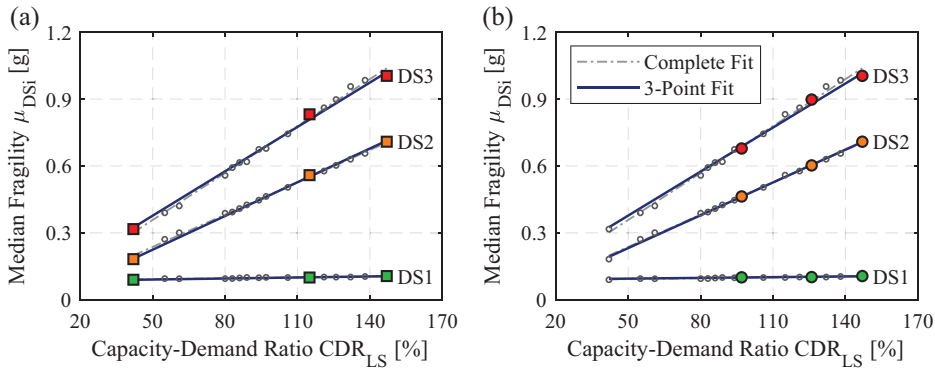
Figure 16. Comparison between the linear models of CDR_{LS} versus μ_{DSi} fitted for the steel jacketing technique using three points considering (a) a first set of points and (b) a second set.

sway configuration as the first point, as indicated by Figure 16b. Nonetheless, using the mixed-sway configuration as the first point is always recommended.

Conclusion

This study proposed a fragility-oriented approach for seismic retrofit design. This approach relies on the mapping between the displacement-based ratio of capacity to life-safety demand (CDR_{LS}), computed using the CSM, and the median of seismic fragility relationships for different damage states. A general, mechanics-based discussion showed that a linear model is a reasonable approximation for such a relationship, which becomes piecewise linear if the adopted retrofit technique produces a sudden shift of the structure's plastic mechanism (e.g. transforming a soft story into a global mechanism). Such a general discussion was empirically demonstrated using an older non-ductile RC frame as a case study, which was retrofitted adopting three widely used techniques: FRP wrapping, steel, and RC jacketing. A large number of retrofit configurations (with varying performance) were developed to populate the CDR_{LS} versus μ_{DSi} space and fit linear trends with R^2 values particularly close to one.

The application of the proposed retrofit design approach only requires defining three points in the CDR_{LS} versus μ_{DS} space, and then deriving the best-fit linear model for those points (for each DS). Accordingly, by specifying a desired fragility median, the designer can obtain the corresponding CDR_{LS} value that will drive the detailed design of the structure. The desired level of fragility can be also linked to seismic risk estimates/loss metrics (e.g. EAL) by using a building-level damage-to-loss model, thus enabling one to indirectly control such metrics. Therefore, using the proposed approach will help avoid the impractical/infeasible process of designing numerous retrofit solutions, carrying out NLTHAs, and finally deriving fragility relationships for each one until ensuring that the acceptable risk (or EAL) level is reached.

Although the illustrative analysis in this article involved a single case study, the empirical data agrees well with the general mechanics-based discussion on the CDR_{LS} versus μ_{DSi} pseudo-linear trend. Therefore, it is reasonable to expect that the proposed fragility-oriented retrofit design approach applies with some level of generality to RC frames, provided that fragility relationships are derived based on the commonly adopted power-law

model, and the CDR_{LS} is displacement-based. Applications to other structural systems and materials must be verified on a case-by-case basis.

ORCID iD

Roberto Gentile https://orcid.org/0000-0002-7682-4490

References

Aboutaha RS, Engelhardt MD, Jirsa JO and Kreger ME (1996) Retrofit of concrete columns with inadequate lap splices by the use of rectangular steel jackets. *Earthquake Spectra* 12(4): 693–714.

Aboutaha RS, Engelhardt MD, Jirsa JO and Kreger ME (1999) Rehabilitation of shear critical concrete columns by use of rectangular steel jackets. *ACI Structural Journal* 96(1): 68–78.

Aljawhari K, Gentile R and Galasso C (2021) Mapping performance-targeted retrofitting to seismic fragility reduction. In: *Proceedings of the 8th international conference on computational methods in structural dynamics and earthquake engineering methods in structural dynamics and earthquake engineering (COMPDYN'2021)*, Athens, 28–30 June, pp. 1301–1321. National Technical University of Athens.

Aljawhari K, Gentile R, Freddi F and Galasso C (2020) Effects of ground-motion sequences on fragility and vulnerability of case-study reinforced concrete frames. *Bulletin of Earthquake Engineering* 19: 6329–6359.

Alvarez JC, Breña SF and Arwade SR (2018) Nonlinear backbone modeling of concrete columns retrofitted with fiber-reinforced polymer or steel jackets. *ACI Structural Journal* 115(1): 53–64.

American Concrete Institute (ACI) 440.2R (2008) *Guide for the Design and Construction of Externally Bonded FRP Systems for Strengthening Concrete Structures* (ACI committee 440). Indianapolis, IN: ACI.

American Society of Civil Engineers (ASCE)/SEI 7-16 (2017) Minimum design loads and associated criteria for buildings and other structures.

American Society of Civil Engineers (ASCE)/SEI 41-17 (2017) Seismic evaluation and retrofit of existing buildings.

Applied Technology Council (ATC)-40 (1996) *Seismic Evaluation and Retrofit of Concrete Buildings*, vol. 1. Redwood City, CA: ATC, 334 pp.

Badoux M and Jirsa JO (1990) Steel bracing of RC frames for seismic retrofitting. *Journal of Structural Engineering: ASCE* 116(1): 55–74.

Baker JW and Cornell CA (2006) Spectral shape, epsilon and record selection. *Earthquake Engineering & Structural Dynamics* 35(9): 1077–1095.

Bousias SN, Biskinis D, Fardis MN and Spathis AL (2007) Strength, stiffness, and cyclic deformation capacity of concrete jacketed members. *ACI Structural Journal* 104(5): 521–531.

Braga F, De Carlo G, Corrado GF, Gigliotti R, Laterza M and Nigro D (2001) Meccanismi di risposta di nodi trave-pilastro in c.a. di strutture non antisismiche. In: *Proceedings of the X Congresso Nazionale "L'ingegneria Sismica in Italia,"* Potenza and Matera, 9–13 September.

Calvi GM, Magenes G and Pampanin S (2002a) Experimental test on a three storey RC frame designed for gravity only. In: *Proceedings of the 12th European conference on earthquake engineering* (paper reference 727), London, 9–13 September.

Calvi GM, Magenes G and Pampanin S (2002b) Relevance of beam-column joint damage and collapse in RC frame assessment. *Journal of Earthquake Engineering* 6(1): 75–100.

Caprili S, Nardini L and Salvatore W (2012) Evaluation of seismic vulnerability of a complex RC existing building by linear and nonlinear modeling approaches. *Bulletin of Earthquake Engineering* 10(3): 913–954.

Cardone D and Perrone G (2015) Developing fragility curves and loss functions for masonry infill walls. *Earthquakes and Structures* 9(1): 257–279.

Cardone D, Gesualdi G and Perrone G (2019) Cost-benefit analysis of alternative retrofit strategies for RC frame buildings. *Journal of Earthquake Engineering* 23(2): 208–241.

Caterino N, Iervolino I, Manfredi G and Cosenza E (2008) Multi-criteria decision making for seismic retrofitting of RC structures. *Journal of Earthquake Engineering* 12(4): 555–583.

Consiglio dei Ministri (1939) *Regulations for the execution of simple and reinforced concrete constructions*. Royal Decree n. 2229, 16 November. Rome: Consiglio dei Ministri (in Italian).

Cornell CA, Jalayer F, Hamburger RO and Foutch DA (2002) Probabilistic basis for 2000 SAC Federal Emergency Management Agency steel moment frame guidelines. *Journal of Structural Engineering: ASCE* 128(4): 526–533.

De Luca F, Woods GED, Galasso C and D'Ayala DF (2018) RC infilled building performance against the evidence of the 2016 EEFIT Central Italy post-earthquake reconnaissance mission: Empirical fragilities and comparison with the FAST method. *Bulletin of Earthquake Engineering* 16(7): 2943–2969.

De Risi MT, Del Gaudio C, Ricci P and Verderame GM (2018) In-plane behaviour and damage assessment of masonry infills with hollow clay bricks in RC frames. *Engineering Structures* 168: 257–275.

Del Gaudio C, De Martino G, Di Ludovico M, Manfredi G, Prota A, Ricci P and Verderame GM (2017) Empirical fragility curves from damage data on RC buildings after the 2009 L'Aquila earthquake. *Bulletin of Earthquake Engineering* 15(4): 1425–1450.

Del Gaudio C, De Risi MT, Ricci P and Verderame GM (2019) Empirical drift-fragility functions and loss estimation for infills in reinforced concrete frames under seismic loading. *Bulletin of Earthquake Engineering* 17: 1285–1330.

EN 1998-1 (2004) Eurocode 8: Design of structures for earthquake resistance—Part 1: General rules, seismic actions and rules for buildings (Authority: The European Union per regulation 305/2011, directive 98/34/EC, directive 2004/18/EC, Brussels).

EN 1998-3 (2005) Eurocode 8: Design of structures for earthquake resistance—Part 3: Assessment and retrofitting of buildings (Authority: The European Union per regulation 305/2011, directive 98/34/EC, directive 2004/18/EC, vol. 1, Brussels).

Federal Emergency Management Agency (FEMA) (2000) Rehabilitation requirements. In: FEMA (ed.) *Prestandard and Commentary for the Seismic Rehabilitation of Buildings*. Washington, DC: FEMA, pp. 1–518.

Freddi F, Ghosh J, Kotoky N and Raghunandan M (2021) Device uncertainty propagation in low-ductility RC frames retrofitted with BRBs for seismic risk mitigation. *Earthquake Engineering & Structural Dynamics* 50: 2488–2509.

Freddi F, Tubaldi E, Ragni L and Dall'Asta A (2013) Probabilistic performance assessment of low-ductility reinforced concrete frames retrofitted with dissipative braces. *Earthquake Engineering & Structural Dynamics* 42: 993–1011.

Freeman SA (1998) Development and use of capacity spectrum method. In: *Proceedings of the 6th US NCEE conference on earthquake engineering/EERI*, Seattle, WA, 31 May–4 June, paper no. 269. Oakland, California: Earthquake Engineering Research Institute.

Gentile R and Galasso C (2020) Gaussian process regression for seismic fragility assessment of building portfolios. *Structural Safety* 87: 101980.

Gentile R and Galasso C (2021a) Simplicity versus accuracy trade-off in estimating seismic fragility of existing reinforced concrete buildings. *Soil Dynamics and Earthquake Engineering* 144: 106678.

Gentile R and Galasso C (2021b) Simplified seismic loss assessment for optimal structural retrofit of RC buildings. *Earthquake Spectra* 37(1): 346–365.

Gentile, R., Galasso, C., Idris, Y., Rusydy, I., and Meilianda, E., 2019. From rapid visual survey to multi-hazard risk prioritisation and numerical fragility of school buildings. *Natural Hazards and Earth System Sciences*, 19(7), 1365–1386. DOI: 10.5194/nhess-19-1365-2019

Gutiérrez-Urzúa F, Freddi F, Di Sarno L, Wu J-R, D'Aniello M, Landolfo R and Bousias S (2021) Preliminary numerical analysis of the seismic response of steel frames with masonry infills retrofitted by buckling-restrained braces. In: *Proceedings of the 8th international conference on computational methods in structural dynamics and earthquake engineering (COMPDYN'2021)*, Athens, 27–30 June, pp. 1506–1518. National Technical University of Athens.

Harrington CC and Liel AB (2020) Evaluation of seismic performance of reinforced concrete frame buildings with retrofitted columns. *Journal of Structural Engineering: ASCE* 146(11): 4020237.

Harrington CC and Liel AB (2021) Indicators of improvements in seismic performance possible through retrofit of reinforced concrete frame buildings. *Earthquake Spectra* 37(1): 262–283.

Jalayer F and Cornell CA (2009) Alternative non-linear demand estimation methods for probability-based seismic assessments. *Earthquake Engineering & Structural Dynamics* 38: 951–972.

Jalayer F, De Risi R and Manfredi G (2015) Bayesian cloud analysis: Efficient structural fragility assessment using linear regression. *Bulletin of Earthquake Engineering* 13: 1183–1203.

Jalayer F, Ebrahimian H, Miano A, Manfredi G and Sezen H (2017) Analytical fragility assessment using unscaled ground motion records. *Earthquake Engineering & Structural Dynamics* 46(15): 2639–2663.

Kaplan H, Yilmaz S, Cetinkaya N and Atimtay E (2011) Seismic strengthening of RC structures with exterior shear walls. *Sadhana: Academy Proceedings in Engineering Sciences* 36(1): 17–34.

Karthik MM and Mander JB (2011) Stress-block parameters for unconfined and confined concrete based on a unified stress-strain model. *Journal of Structural Engineering: ASCE* 137(2): 270–273.

Kazantziazantzi AK and Vamvatsikos D (2015) Intensity measure selection for vulnerability studies of building classes. *Earthquake Engineering & Structural Dynamics* 44(15): 2677–2694.

Kohrangi M, Bazzurro P and Vamvatsikos D (2016) Vector and scalar IMs in structural response estimation, Part II: Building demand assessment. *Earthquake Spectra* 32(3): 1525–1543.

Kohrangi M, Bazzurro P, Vamvatsikos D and Spillatura A (2017) Conditional spectrum-based ground motion record selection using average spectral acceleration. *Earthquake Engineering & Structural Dynamics* 46(10): 1667–1685.

Lam L and Teng JG (2003) Design-oriented stress–Strain model for FRP-confined concrete. *Construction and Building Materials* 17(6–7): 471–489.

Liel AB and Deierlein GG (2013) Cost-benefit evaluation of seismic risk mitigation alternatives for older concrete frame buildings. *Earthquake Spectra* 29(4): 1391–1411.

Ligabue V, Pampanin S and Savoia M (2018) Seismic performance of alternative risk-reduction retrofit strategies to support decision making. *Bulletin of Earthquake Engineering* 16(7): 3001–3030.

Lizundia B, Holmes WT, Cobeen K, Malley J and Lew HS (2006) Techniques for the seismic rehabilitation of existing buildings. In: *Proceedings of the 8th US National conference on earthquake engineering*, San Francisco, CA, 18–22 April, pp. 3646–3656. Earthquake Engineering Research Institute (EERI).

McKenna F (2011) OpenSees: A framework for earthquake engineering simulation. *Computing in Science & Engineering* 13(4): 58–66.

Mander JB, Priestley MJN and Park R (1988) Theoretical stress-strain model for confined concrete. *Journal of Structural Engineering: ASCE* 114(8): 1804–1826.

Masi A, Digrisolo A and Santarsiero G (2014) Concrete strength variability in Italian RC buildings: Analysis of a large database of core tests. *Applied Mechanics and Materials* 597: 283–290.

Mazzoni S, Castori G, Galasso C, Calvi P, Dreyer R, Fischer E, Fulco A, Sorrentino L, Wilson J, Penna A and Magenes G (2018) 2016–2017 Central Italy earthquake sequence: Seismic retrofit policy and effectiveness. *Earthquake Spectra* 34(4): 1671–1691.

Mergos PE and Kappos AJ (2012) A gradual spread inelasticity model for R/C beam–Columns, accounting for flexure, shear and anchorage slip. *Engineering Structures* 44: 94–106.

Miano A, Sezen H, Jalayer F and Prota A (2017) Performance-based comparison of different retrofit methods for reinforced concrete sructures. In: *Proceedings of the 6th international conference on computational methods in structural dynamics and earthquake engineering (COMPDYN'2017)*, Rhodes Island, 15–17 June, vol. 1, pp. 1515–1535. National Technical University of Athens.

Minas S and Galasso C (2019) Accounting for spectral shape in simplified fragility analysis of case-study reinforced concrete frames. *Soil Dynamics and Earthquake Engineering* 119: 91–103.

Natale A, Del Vecchio C and Di Ludovico M (2021) Seismic retrofit solutions using base isolation for existing RC buildings: Economic feasibilty and pay-back time. *Bulletin of Earthquake Engineering* 19(1): 483–512.

National Research Council (CNR)-DT 200 R1/2013 (2013) Guide for the design and construction of externally bonded FRP systems for strengthening existing structures: Materials, RC and PC structures, masonry structures.

Nettis A, Gentile R, Raffaele D, Uva G and Galasso C (2021) Cloud Capacity Spectrum Method: Accounting for record-to-record variability in fragility analysis using nonlinear static procedures. *Soil Dynamics and Earthquake Engineering* 150: 106829.

New Zealand Society for Earthquake Engineering (NZSEE) (2006) *Assessment and Improvement of the Structural Performance of Buildings in Earthquakes*. Wellington, New Zealand: NZSEE.

O'Reilly GJ (2021) Limitations of Sa(T1) as an intensity measure when assessing non-ductile infilled RC frame structures. *Bulletin of Earthquake Engineering* 19(6): 2389–2417.

O'Reilly GJ and Sullivan TJ (2018) Probabilistic seismic assessment and retrofit considerations for Italian RC frame buildings. *Bulletin of Earthquake Engineering* 16: 1447–1485.

O'Reilly GJ and Sullivan TJ (2019) Modeling techniques for the seismic assessment of the existing Italian RC frame structures. *Journal of Earthquake Engineering* 23(8): 1262–1296.

Pampanin S, Calvi GM and Moratti M (2002) Seismic behaviour of R.C. beam-column joints designed for gravity loads. In: *Proceedings of the 12th European conference on earthquake engineering* (paper reference 726), London, 9–13 September.

Pampanin S, Magenes G and Carr A (2003) Modelling of shear hinge mechanism in poorly detailed RC beam-column joints. In: *Proceedings of the fib symposium 2003: Concrete structures in seismic regions*, Athens, 6–8 May, paper no. 171. Athens: Technical Chamber of Greece.

Priestley MJN (1997) Displacement-based seismic assessment of reinforced concrete buildings. *Journal of Earthquake Engineering* 1: 157–192.

Priestley MJN and Seible F (1995) Design of seismic retrofit measures for concrete and masonry structures. *Construction and Building Materials* 9(6): 365–377.

Priestley MJN, Calvi GM and Kowalsky MJ (2007) *Displacement Based Seismic Design of Structures*. Pavia: Fondazione EUCENTRE, IUSS Press.

Priestley MJN, Seible F and Calvi GM (1996) *Seismic Design and Retrofit of Bridges*. New York: Wiley.

Priestley MJN, Seible F, Xiao Y and Verma R (1994) Steel jacket retrofitting of reinforced concrete bridge columns for enhanced shear strength. Part 2: Test results and comparison with theory. *ACI Materials Journal* 91(5): 537–551.

Puppio ML, Pellegrino M, Giresini L and Sassu M (2017) Effect of material variability and mechanical eccentricity on the seismic vulnerability assessment of reinforced concrete buildings. *Buildings* 7(3): 66.

Ricci P, De Luca F and Verderame GM (2011) 6th April 2009 L'Aquila earthquake, Italy: Reinforced concrete building performance. *Bulletin of Earthquake Engineering* 9: 285–305.

Rodriguez M and Park R (1994) Seismic load tests on reinforced concrete columns strengthened by jacketing. *ACI Structural Journal* 91(2): 150–159.

Rosti A, Del Gaudio C, Rota M, Ricci P, Di Ludovico M, Penna A and Verderame GM (2021) Empirical fragility curves for Italian residential RC buildings. *Bulletin of Earthquake Engineering* 19(8): 3165–3183.

Sassun K, Sullivan TJ, Morandi P and Cardone D (2016) Characterising the in-plane seismic performance of infill masonry. *Bulletin of the New Zealand Society for Earthquake Engineering* 49(1): 100–117.

Seible F, Priestley MJN, Hegemier GA and Innamorato D (1997) Seismic retrofit of RC columns with continuous carbon fiber jackets. *Journal of Composites for Construction* 1(2): 52–62.

Sezen H and Moehle JP (2004) Shear strength model for lightly reinforced concrete columns. *Journal of Structural Engineering: ASCE* 130(11): 1692–1703.

Silva V, Amo-Oduro D, Calderon A, Dabbeek J, Despotaki V, Martins L, Rao A, Simionato M, Viganoä D, Yepes-Estrada C, Acevedo A, Crowley H, Horspool N, Jaiswal K, Journeay M and Pittore M (2018) Global earthquake model (GEM) seismic risk map (version 2018.1; This work is licensed under the terms of the Creative Commons Attribution- NonCommercial-ShareAlike 4.0 International License (CC BY-NC-SA)). Available at: https://www.globalquakemodel.org/gem-maps/global-earthquake-risk-map (accessed on 4 April 2021).

Smerzini C, Galasso C, Iervolino I and Paolucci R (2014) Ground motion record selection based on broadband spectral compatibility. *Earthquake Spectra* 30(4): 1427–1448.

Stewart JP, Zimmaro P, Lanzo G, Mazzoni S, Ausilio E, Aversa S, Bozzoni F, Cairo R, Capatti MC, Castiglia M, Chiabrando F, Chiaradonna A, d'Onofrio A, Dashti S, De Risi R, de Silva F, Pasqua FD, Dezi F, Di Domenica A, Di Sarno L, Durante MG, Falcucci E, Foti S, Franke KW, Galadini F, Giallini S, Gori S, Kayen RE, Kishida T, Lingua A, Lingwall B, Mucciacciaro M, Pagliaroli A, Passeri F, Pelekis P, Pizzi A, Reimschiissel B, Santo A, de Magistris FS, Scasserra G, Sextos A, Sica S, Silvestri F, Simonelli AL, Spanò A, Tommasi P and Tropeano G (2018) Reconnaissance of 2016 Central Italy earthquake sequence. *Earthquake Spectra* 34(4): 1547–1555.

Vamvatsikos D and Cornell CA (2002) Incremental dynamic analysis. *Earthquake Engineering & Structural Dynamics* 31(3): 491–514.

Verderame GM, Polese M, Mariniello C and Manfredi G (2010) A simulated design procedure for the assessment of seismic capacity of existing reinforced concrete buildings. *Advances in Engineering Software* 41(2): 323–335.

Verderame GM, Stella A and Cosenza E (2001) Le proprietà meccaniche degli acciai impiegati nelle strutture in c.a. realizzate negli anni '60. In: *Proceedings of the X Congresso Nazionale "L'ingegneria Sismica in Italia,"* Potenza and Matera, 9–13 September.

Zimos DK, Mergos PE and Kappos AJ (2015) Shear hysteresis model for reinforced concrete elements including the post-peak range. In: *Proceedings of the 5th ECCOMAS thematic conference on computational methods in structural dynamics and earthquake engineering (COMPDYN'2015)*, Crete Island, 25–27 May, pp. 2640–2658. National Technical University of Athens.